On the role of coherence in the transition from kinetics to dynamics: Theory and application to femtosecond unimolecular reactions

Klaus B. Møller, Niels E. Henriksen, and Ahmed H. Zewail

Citation: The Journal of Chemical Physics **113**, 10477 (2000); doi: 10.1063/1.1323729
View online: http://dx.doi.org/10.1063/1.1323729
View Table of Contents: http://scitation.aip.org/content/aip/journal/jcp/113/23?ver=pdfcov
Published by the AIP Publishing

On the role of coherence in the transition from kinetics to dynamics: Theory and application to femtosecond unimolecular reactions

Klaus B. Møller, Niels E. Henriksen,[a] and Ahmed H. Zewail[b]
Arthur Amos Noyes Laboratory of Chemical Physics, California Institute of Technology, Pasadena, California 91106

(Received 17 August 2000; accepted 19 September 2000)

We consider the relation between observed pump–probe signals in the femtosecond regime and the kinetics of unimolecular reactions, that is, the exponential decay of reactants and the exponential rise of the product population, respectively. It is shown that the signals cannot be fully accounted for within standard approaches of unimolecular decay, conventionally used in the past, since *interference effects* between the quasi-bound vibrational states within the bandwidth of the pump laser cannot be neglected. When these effects are included, all features of the signals can be accounted for. We apply this theoretical treatment of coherent interference to examine the dynamics and kinetics of the quasi-bound transition configurations, and relate them to the decay rates of individual quasi-bound resonance states. The signals show multi-exponential behavior, reflecting the different decay rates of the resonance states, with an average rate constant (within the bandwidth of the pump laser) which can be extracted directly from the signals. The persistence of coherence is evident in the observed signals. The predissociation of NaI is used as a prototype for numerical illustration. © *2000 American Institute of Physics.* [S0021-9606(00)70747-1]

I. INTRODUCTION

The field of reaction kinetics is concerned with the description of chemical reactions in terms of rate processes and the assignment of (macroscopic) rate constants to the involved transformations. In the case of a unimolecular reaction, for instance, the decay of the reactants is often modeled by simple first-order rate laws. However, the study of chemical reactions on the molecular level, that is, in terms of nuclear motion, is the key to the understanding of the dynamics of the transformation and, hence, provides physical insight complimentary to the more phenomenological kinetic description. The dynamics of elementary physical and chemical processes can be followed in real time using femtosecond (fs) laser pump–probe techniques.[1–6] A fs pump pulse coherently excites (activates) the molecular system under consideration and another fs pulse subsequently probes the system at various instants as it undergoes the transformation. The obtained pump–probe signal thus records the molecular rearrangement during the course of the process.

In this paper, we consider the theoretical relation between pump–probe signals and reaction kinetics for unimolecular reactions. The reaction dynamics of photoactivated molecular reactions are naturally described theoretically by the time evolution of a wave packet, obtained by solving the time-dependent Schrödinger equation, or by classical trajectory calculations.[6–8] Alternatively, if the reaction involves the decay of a meta-stable intermediate, a microscopic description of the dynamics in terms of the decay of quasi-bound resonance states can be invoked.[7,8] Adopting such a description we derive explicit expressions for the pump–probe signals for molecules which undergo unimolecular reaction in order to make contact with reaction characteristics, lifetimes and rate constants, and ultimately with reaction kinetics.

Because the ultrashort pulse excites several resonance states coherently, the approach most commonly used in the past, where each resonance state decays independently,[7–12] is inadequate in this context. The coupling between different resonance-state amplitudes must be taken into account.[13] Here, we treat this problem of resonance decay in coherently prepared reactions. The derived expressions clearly display the coherence induced by the laser excitation as well as the connection between pump–probe signals and unimolecular rate constants associated with the individual resonance states. If detailed information about the individual resonances is not needed, that is, a unimolecular rate constant averaged over a narrow energy range suffices, we suggest how to extract such a rate constant directly from a pump–probe signal. We exemplify our results with numerical simulations of the predissociation dynamics of NaI. This reaction is a prototype and has already been studied extensively both experimentally[14–18] and theoretically, using semiclassic and quantal calculations.[19–24]

This paper is organized in the following way: In Sec. II, we summarize some of the general expressions for pump–probe signals. In Sec. III, the dynamics of unimolecular decay is discussed in terms of quasi-bound resonance states. The relation between the pump–probe signals and the decay rates of individual vibrational states is discussed. In Sec. IV, we analyze, as an example, the pump–probe signals of NaI, and their relation to reaction kinetics. Finally, in Sec. V the conclusions of our work are summarized.

[a]Permanent address: Department of Chemistry, Technical University of Denmark, DTU 207, DK-2800 Lyngby, Denmark.
[b]Electronic mail: zewail@caltech.edu

II. PUMP–PROBE SIGNALS, GENERAL EXPRESSIONS

We consider the interaction between a molecule and two time-delayed pulses—a pump and a probe pulse. Within the electric dipole approximation, the field-molecule coupling terms take the form (for absorption)

$$V_{\text{pump}}(t) = -(\tfrac{1}{2})\mu_{10}a_1(t)e^{-i\omega_1 t},$$

$$V_{\text{probe}}(t) = -(\tfrac{1}{2})\mu_{21}a_2(t)e^{-i\omega_2 t}, \tag{1}$$

where ω_1 and ω_2 are the carrier frequencies, μ_{10} and μ_{21} are the projections of the transition dipole moments on the polarization of the electric field vector, and $a_1(t)$ and $a_2(t)$ are the pulse envelopes centered around time zero and the delay time t_d, respectively.

The pump pulse creates a wave packet $|\psi_1(t)\rangle$ in electronic state (1) which is evaluated according to first-order perturbation theory, and $\hat{H}_1$ is the Hamiltonian for nuclear motion in this electronic state. The probe pulse creates a new nonstationary state $|\psi_2(t)\rangle$ in electronic state (2). In the limit of nonoverlapping pump and probe pulses, which we will consider in the present paper, this state can again be calculated according to first-order perturbation theory, now with $|\psi_1(t)\rangle$ as initial state.

The total pump–probe signal is assumed to be proportional to the norm of $|\psi_2(t)\rangle$ after the probe pulse has decayed to zero. It can be written as a function of the delay time, t_d, in the following form:[25]

$$S(t_d) = \langle \psi_1(t_d)|\hat{\mathcal{P}}_{12}(\omega_2)|\psi_1(t_d)\rangle, \tag{2}$$

where $\hat{\mathcal{P}}_{12}(\omega_2)$ is the probe operator

$$\hat{\mathcal{P}}_{12}(\omega_2) = \hat{P}^{\dagger}(\omega_2)\hat{P}(\omega_2), \tag{3}$$

with

$$\hat{P}(\omega_2) = (1/\hbar)\int_{-\infty}^{\infty} e^{-i\omega_2 t}a_2(t)\exp(i\hat{H}_2 t/\hbar)\mu_{21} \times \exp(-i\hat{H}_1 t/\hbar)dt. \tag{4}$$

For an ultrashort probe pulse where $a_2(t)$ is strongly peaked around $t=t_d$, and under the assumption that the transition dipole moment is coordinate independent, the signal can be written in the form[26–28]

$$S(t_d) = \int d\mathbf{q}\psi_1^*(\mathbf{q},t_d)|F[D(\mathbf{q})-\omega_2]|^2\psi_1(\mathbf{q},t_d) = \int d\mathbf{q}|F[D(\mathbf{q})-\omega_2]|^2|\psi_1(\mathbf{q},t_d)|^2, \tag{5}$$

where we have introduced the Franck–Condon window function

$$|F[D(\mathbf{q})-\omega_2]|^2 = \left|\mu_{21}\int_{-\infty}^{+\infty} dt a_2(t)e^{i[D(\mathbf{q})-\hbar\omega_2]t/\hbar}\right|^2. \tag{6}$$

Here $\mathbf{q}$ denotes the collection of all nuclear coordinates, and $D(\mathbf{q}) = V_2(\mathbf{q}) - V_1(\mathbf{q})$ is the difference between the potential energy surfaces in the electronic states (2) and (1). Thus, the signal measures the square magnitude of the wave packet ψ_1 within the Franck–Condon window at time t_d. We note that this is an overlap between two densities, i.e., not wave functions.

Consider, as an example, a Gaussian probe pulse $a_2(t) = \sqrt{\gamma/\pi}E_0\exp[-\gamma(t-t_d)^2]$. The Franck–Condon window takes the form

$$|F[D(\mathbf{q})-\omega_2]|^2 = E_0^2|\mu_{21}|^2 e^{-[\omega_2 - D(\mathbf{q})/\hbar]^2/(2\gamma)}. \tag{7}$$

In order to gain insight, we consider now one coordinate and linearize the difference potential around the ''Franck–Condon point,'' $r=r_0$, where $\hbar\omega_2 = D(r_0)$. Thus,

$$D(r) = D(r_0) + g(r-r_0), \tag{8}$$

where $g = D'_{r=r_0}$ is the derivative of the difference potential (note that the equation $\hbar\omega_2 = D(r_0)$ may have more than one solution). Equation (7) now takes the form

$$|F[D(r)-\omega_2]|^2 = E_0^2|\mu_{21}|^2 e^{-(g/\hbar)^2(r-r_0)^2/(2\gamma)}. \tag{9}$$

Thus, the probe window is a Gaussian around the Franck–Condon point. The position of this point depends on the probe frequency ω_2.

If the probe pulse is very short ($\gamma\to\infty$), or equivalently $g\to 0$, the probe becomes insensitive to the potential energy difference. In this limit, the window is essentially a constant over the width of the wave packet at all times. Hence, $S(t_d)\to|\mu_{21}|^2\langle\psi_1(t_d)|\psi_1(t_d)\rangle$; the signal is proportional to the norm of the wave packet, which in a chemical reaction exhibits an overall decay, see Sec. III.

Finally, it is instructive to consider the relation between the pump–probe signal (for transition states) and the cross-correlation function,

$$C(t) = |\langle\psi_p|\psi_1(t)\rangle|^2 = \langle\psi_1(t)|\psi_p\rangle\langle\psi_p|\psi_1(t)\rangle = \int\int d\mathbf{q}d\mathbf{q}'\,\psi_1^*(\mathbf{q}',t)\psi_p(\mathbf{q}')\psi_p^*(\mathbf{q})\psi_1(\mathbf{q},t), \tag{10}$$

where $|\psi_p\rangle$ is an arbitrary ''probe state.'' Hence, $C(t)$ can be interpreted as the expectation value of the projection operator $|\psi_p\rangle\langle\psi_p|$. This function is quite similar to Eq. (2) which is perhaps most transparent in the limit of a short probe pulse as in Eq. (5). The ''projection operator'' in Eq. (5) is, however, even simpler, since it is diagonal in $\mathbf{q}$. The relation between the cross-correlation function and the pump–probe signal in Eq. (5) can be even more clearly expressed in phase space. In the Wigner phase-space representation,[29,30] the cross-correlation takes the form

$$C(t) = \int\int d\mathbf{q}d\mathbf{p}W_{\psi_p}(\mathbf{q},\mathbf{p})W_{\psi_1}(\mathbf{q},\mathbf{p},t), \tag{11}$$

where $W_{\psi_p}(\mathbf{q},\mathbf{p})$ and $W_{\psi_1}(\mathbf{q},\mathbf{p},t)$ are the Wigner functions corresponding to the $|\psi_p\rangle$ and $|\psi_1(t)\rangle$ states, respectively. If the probe state is highly localized in configuration space, and therefore almost constant in momentum space, the cross-correlation function reduces to

$$C(t)\sim \int d\mathbf{q} W_{\omega_p}(\mathbf{q}) \int d\mathbf{p} W_{\psi_1}(\mathbf{q},\mathbf{p},t)$$

$$= \int d\mathbf{q} W_{\psi_p}(\mathbf{q}) |\psi_1(\mathbf{q},t)|^2. \quad (12)$$

Thus, an expression similar to the one for the pump–probe signal is recovered in the limit where the probe state is very broad (constant) in momentum space. Since the pump–probe signal is not sensitive to the momentum, the cross-correlation function is, in general, expected to show more structure than the pump–probe signal. In many cases, however, the probe state will be sufficiently localized such that $C(t)$ is a good measure of a pump–probe signal.

III. DYNAMICS OF UNIMOLECULAR DECAY

In order to make contact with observables such as lifetimes, rate constants, and ultimately reaction kinetics, we begin with the dynamics in terms of the decay of resonance states.

A. Decay of resonance states

For unimolecular decay, the state created by the pump pulse, $|\psi_1(0)\rangle$, is in the ''bound'' region of the potential energy surface. We now expand this state in zero-order resonance states (states with finite lifetime) which are *weakly coupled* to continuum states $|E'\rangle$ (which we for simplicity assume to be nondegenerate). Thus,

$$|\psi_1(0)\rangle = \sum_n c_n |n\rangle, \quad (13)$$

where

$$\sum_n |c_n|^2 = 1. \quad (14)$$

The coefficients c_n are determined by the pump pulse. For a δ-pump pulse the square magnitude of these coefficients follow a Poisson distribution (in the harmonic coherent state limit) which is often well approximated by a Gaussian distribution.

In standard derivations (see, e.g., Refs. 7–12), the decays of the individual resonance states are uncoupled. Here we wish to include possible interferences between decays when several states are coherently excited and proceed along the lines of the treatment presented in Ref. 13. Since the resonance states are not eigenstates of the full Hamiltonian, the time-dependent state, $|\psi_1(t)\rangle$, is expanded in both the resonance and the continuum states

$$|\psi_1(t)\rangle = \sum_n c_n(t)|n\rangle + \int dE' h(E';t)|E'\rangle. \quad (15)$$

The dynamics of the ''bound'' part, i.e., the time evolution of the amplitudes $c_1(t), c_2(t), \ldots, c_n(t)$, can be formulated in terms of the effective (non-Hermitian) Hamiltonian[13]

$$\mathbf{H}_{\text{eff}} = \mathbf{H}_0 - \frac{i\hbar}{2}\boldsymbol{\Gamma}, \quad (16)$$

where $\mathbf{H}_0$ is the diagonal matrix

$$(\mathbf{H}_0)_{nn'} = E_n \delta_{nn'}, \quad (17)$$

and $\boldsymbol{\Gamma}$ is the decay matrix

$$(\boldsymbol{\Gamma})_{nn'} \equiv \Gamma_{nn'} = \frac{2\pi}{\hbar}\langle V_{nE'} V_{E'n'}\rangle \rho(\bar{E}_{nn'}). \quad (18)$$

Here $V_{nE'}$ denotes the coupling matrix element between the resonance state $|n\rangle$ and the continuum state $|E'\rangle$, and $\langle V_{nE'} V_{E'n'}\rangle$ is the average over a (narrow) energy range around $\bar{E}_{nn'} = (E_n + E_{n'})/2$, including both E_n and $E_{n'}$

$$\langle V_{nE'} V_{E'n'}\rangle = \frac{1}{\rho(\bar{E}_{nn'})} \int dE' V_{nE'} V_{E'n'} \times \rho(E')\,\delta_\epsilon(E' - \bar{E}_{nn'}). \quad (19)$$

Hence $\Gamma_{nn'} = \Gamma_{n'n}$ and the decay matrix is a symmetric real matrix. The diagonal element, $\Gamma_{nn} \equiv \Gamma_n$, is the width of the nth resonance state or, equivalently, determines its lifetime, $\tau_n = \hbar/\Gamma_n$. The physical significance of the off-diagonal elements is more subtle[13] and for now it suffices to assume that they are of the same order of magnitude as the diagonal elements (a more quantitative statement of this assumption is given below). It should be noted that static inhomogeneous broadening effects on the energy differences has been neglected.[13]

With these definitions, $\mathbf{c}(t) \equiv [c_1(t), c_2(t), \ldots, c_n(t)]$ satisfies the equation of motion

$$i\hbar \frac{d}{dt}\mathbf{c}(t) = \mathbf{H}_{\text{eff}}\mathbf{c}(t), \quad (20)$$

with the initial condition $\mathbf{c}(t) = \mathbf{c}$. The formal solution to Eq. (20) takes the form

$$\mathbf{c}(t) = \exp(-i\mathbf{H}_{\text{eff}} t/\hbar)\mathbf{c}. \quad (21)$$

Apart from solving this equation numerically, it is illustrative to consider the situation of nonoverlapping resonances ($\Gamma_{nn'} \ll |E_n - E_{n'}|$). In this limit, the analytical solution is found to be

$$c_n(t) = \left\{ c_n - \sum_{n' \neq n} c_{n'} \frac{i k_{nn'}}{2\omega_{nn'}} \times [1 - e^{i\omega_{nn'}t} e^{(k_n - k_{n'})t/2}] \right\} e^{-iE_n t/\hbar} e^{-k_n t/2}, \quad (22)$$

where we have introduced the symbols

$$\omega_{nn'} \equiv (E_n - E_{n'})/\hbar,$$

$$k_{nn'} \equiv \Gamma_{nn'}/\hbar, \quad (23)$$

$$k_n \equiv \Gamma_n/\hbar.$$

Equation (22) shows indeed that the resonance states do not decay independently. To first order in the quantity $k_{nn'}/\omega_{nn'}$, this gives the following expression for the norm:

$$\langle\psi_1(t)|\psi_1(t)\rangle=\sum_n |c_n|^2 e^{-k_n t}-\sum_n \sum_{n'\neq n} |c_n||c_{n'}|\frac{k_{nn'}}{\omega_{nn'}} \times\{\sin(\omega_{nn'}t-\varphi_{nn'})e^{-(k_n+k_{n'})t/2} +\sin(\varphi_{nn'})e^{-k_n t}\}, \tag{24}$$

where $\varphi_{nn'}=\arg(c_n)-\arg(c_{n'})$.

For practical purposes the widths are determined by standard techniques[31–33] and the off-diagonal elements can be assigned the values

$$\Gamma_{nn'}=\eta_{nn'}\sqrt{\Gamma_n\Gamma_{n'}}, \tag{25}$$

where $\eta_{nn'}$ is a number between 0 and 1.[13]

The off-diagonal terms in Eq. (24) correspond to an oscillatory modulation in the overall decay. In order to make contact with reaction kinetics, we consider now the average value of these terms measured over an oscillation period, assuming that the relevant energy levels are equidistantly spaced, i.e., $\omega_{nn'}=(n-n')\omega$. The average value can be evaluated as the integral over a period divided by the length of the period

$$\int_{nT+t_0}^{(n+1)T+t_0}\sin(\omega_{nn'}t-\varphi_{nn'})e^{-(k_n+k_{n'})t/2}dt =\exp[-t_0(k_n+k_{n'})/2] \times\exp[-nT(k_n+k_{n'})/2]\frac{\omega_{nn'}[1-e^{-T(k_n+k_{n'})/2}]}{(\omega_{nn'})^2+[(k_n+k_{n'})/2]^2}, \tag{26}$$

where $T=2\pi/\omega$ is the fundamental period of the oscillation and $t_0=\varphi_{nn'}/\omega_{nn'}$. Thus, the average value of this term is zero in the limit $(k_n+k_{n'})/2\ll\omega$, which is the limit of nonoverlapping resonances considered in Eq. (24). The time average of the last term in Eq. (24) gives a number proportional to $\exp[-k_n nT](\exp[-k_n T]-1)\sin(\varphi_{nn'})$. That is, the time-averaged norm is, except for a possible shift which depends on the phase relation between the coefficients and which vanish at long times, identical to the norm which is obtained when the coupling between the decays of the resonance states is neglected. Now using Eq. (22) in this limit, the dynamics is given by

$$|\psi_1(t)\rangle=\sum_n c_n|n\rangle e^{-iE_n t/\hbar}e^{-k_n t/2}, \tag{27}$$

which implies

$$\langle\psi_1(t)|\psi_1(t)\rangle=\sum_n |c_n|^2 e^{-k_n t}, \tag{28}$$

corresponding to a decay given by a superposition of exponential decays. In light of the above discussion, Eq. (28) reflects the ''average population'' in the quasi-bound region of the potential.

B. Pump–probe signals

In this section we combine the results of the previous sections in order to obtain expressions for the signal one would obtain in a pump–probe experiment. The simplest signal is obtained by merely monitoring the formation of products. The product signal is given by

$$P(t)=1-\langle\psi_1(t)|\psi_1(t)\rangle, \tag{29}$$

where it is assumed that all population which is not in the quasi-bound part of the potential is detected as products, and where the norm is given by Eq. (24). If we instead use the approximate expression in Eq. (28), the product signal is just given by superposition of exponential rises

$$P(t)=1-\sum_n |c_n|^2 e^{-k_n t}. \tag{30}$$

As already argued, this approximation is reasonable when *the signal is not resolved on the time scale of vibrational periods*. In this limit the product signal corresponds to a multiexponential rise, which reflects the decay rates of the resonance states. Equations (24) and (28) also give the pump–probe signal for the quasi-bound states in the limit where the probe operator is independent of the nuclear coordinates, i.e., proportional to the identity operator.

We consider now the general expression for the pump–probe signal for the quasi-bound states. We evaluate explicitly the expression for the pump–probe signal for the detection of transition states, with a quantum state of the form given in Eq. (27). In this case the wave function becomes

$$\psi_1(\mathbf{q},t)=\sum_n c_n\phi_n(\mathbf{q})e^{-iE_n t/\hbar}e^{-k_n t/2}, \tag{31}$$

where $\phi_n(\mathbf{q})=\langle\mathbf{q}|n\rangle$. Hence,

$$|\psi_1(\mathbf{q},t)|^2=\sum_n |c_n|^2\phi_n(\mathbf{q})^2e^{-k_n t} +2\sum_n\sum_{n'<n}|c_n||c_{n'}|\phi_n(\mathbf{q})\phi_{n'}(\mathbf{q}) \times\cos(\omega_{nn'}t-\varphi_{nn'})e^{-(k_n+k_{n'})t/2}, \tag{32}$$

where we have assumed that $\phi_n(\mathbf{q})$ is real valued. Inserting this into Eq. (5) we obtain

$$S(t)=\sum_n |c_n|^2 A_n e^{-k_n t}+2\sum_n\sum_{n'<n}|c_n||c_{n'}|B_{nn'} \times\cos(\omega_{nn'}t-\varphi_{nn'})e^{-(k_n+k_{n'})t/2}, \tag{33}$$

where

$$A_n=\int d\mathbf{q}|F(D(\mathbf{q})-\omega_2)|^2\phi_n(\mathbf{q})^2, \qquad B_{nn'}=\int d\mathbf{q}|F(D(\mathbf{q})-\omega_2)|^2\phi_n(\mathbf{q})\phi_{n'}(\mathbf{q}). \tag{34}$$

Equation (33) shows that the pump–probe signal for the transition states consists of resonance recurrences damped by the unimolecular decay. We remind the reader that this expression includes the (quantum) interference between the quasi-bound states but assumes that each of them decays exponentially (cf. Ref. 9).

It is illustrative to evaluate the cross-correlation function in Eq. (10), where $|\psi_p\rangle$ is chosen such that the bound region of the potential is probed. With

$$|\psi_p\rangle = \sum_n b_n |n\rangle, \tag{35}$$

the cross-correlation function takes the form

$$C(t) = \left| \sum_n b_n^* c_n e^{-iE_n t/\hbar} e^{-k_n t/2} \right|^2. \tag{36}$$

Depending on the form of $|\psi_1(0)\rangle$ as well as the probe state, $C(t)$ can be dominated by one or more resonances. The autocorrelation function (where $c_n = b_n$) can be written in the form

$$\begin{aligned} C(t) &= \left| \sum_n |c_n|^2 e^{-iE_n t/\hbar} e^{-k_n t/2} \right|^2 \\ &= \sum_n \sum_{n'} |c_n|^2 |c_{n'}|^2 e^{-(k_n + k_{n'})t/2} e^{i\omega_{nn'} t} \\ &= \sum_n |c_n|^4 e^{-k_n t/\hbar} \\ &\quad + 2 \sum_n \sum_{n'<n} |c_n|^2 |c_{n'}|^2 \cos(\omega_{nn'} t) e^{-(k_n + k_{n'})t/2}. \end{aligned} \tag{37}$$

Thus, the pump–probe signal in Eq. (33) and the auto-/cross-correlation function have the same form of time dependence, and for the purpose of making contact with reaction kinetics, we can consider the autocorrelation function without loss of generality.

In the special case where all resonance states have the same decay rates, i.e., if $k_n = k$ for all n, then

$$\begin{aligned} C(t) = e^{-kt} \Bigg\{ & \sum_n |c_n|^4 \\ & + 2 \sum_n \sum_{n'<n} |c_n|^2 |c_{n'}|^2 \cos(\omega_{nn'} t) \Bigg\}. \end{aligned} \tag{38}$$

Thus, in this case the unimolecular decay and the resonance recurrences factorize. The quantity in the curly brackets corresponds to the autocorrelation function without unimolecular decay, whereas the exponential prefactor corresponds to the unimolecular decay. Hence $C(t)\exp(kt)$ provides information on the spreading and recurrences of the wave packet in the bound region of the potential, separated from the unimolecular decay, cf. Ref. 34. In a bound potential the decay of peak heights in the autocorrelation function, within the first few vibrational periods, is a signature of the wave packet spreading on this time scale. That is, from the signal and the unimolecular decay rate, information on the spreading of the wave packet can be obtained [see also the discussion following Eq. (40)].

Another simple illustration of the connection between the signal and the decay rates is for two resonances, where the autocorrelation function takes the form

$$\begin{aligned} C(t) &= c_1^4 e^{-k_1 t/\hbar} + c_2^4 e^{-k_2 t/\hbar} \\ &\quad + 2 c_1^2 c_2^2 \cos(\omega_{nn'} t) e^{-(k_1 + k_2)t/2}. \end{aligned} \tag{39}$$

Here, it is important to stress that not even the *average* decay rate, $\langle k \rangle = (k_1 + k_2)/2$ is related to the overall decay (envelope function) except when the decay rates are very similar.

In general, from the signal (or autocorrelation function), we desire to extract decay rates. That is, from the observed decay of the signal, we wish to separate the contribution due to the loss of coherence (spreading) in an anharmonic potential from that due to unimolecular decay. It should be noted that the state specific decay rate can be extracted numerically—at least in principle—from $C(t)$.[35] However, it is useful to have a simple scheme in order to extract kinetic information directly form the pump–probe signal. To that end, we note that with the window given in Eq. (9) and within the Gaussian wave packet approximation,[36,37] the signal can be written in the form

$$\begin{aligned} S(t) = & \frac{E_0^2 |\mu_{21}|^2}{4\hbar^2} \sqrt{\frac{2\gamma}{2(\Delta r)_t^2 (g/\hbar)^2 + 2\gamma}} \\ & \times \exp\left[- \frac{(g/\hbar)^2}{2(\Delta r)_t^2 (g/\hbar)^2 + 2\gamma} (r_t - r_0)^2 \right], \end{aligned} \tag{40}$$

where r_t and $(\Delta r)_t$ are the expectation value and uncertainty, respectively, of the position of the wave packet at time t. From this equation we observe that the *peak height* will decay as the packet spreads, whereas the *area* under each peak—given as peak height times the width—is constant. Assuming again that all resonance states have the same decay rates, the peak areas should decay exponentially in this limit. In general, we expect that the areas decay in the same way as the norm of the wave packet. We will return to this proposition in the next section. It is clear from the above discussion, that it is simpler to analyze the connection to reaction kinetics from the rise of the product signal, Eq. (29), since this signal is (essentially) free of wave packet spreading.

Finally, it should be stressed that the discussion in this section concerns standard unimolecular decay, that is *indirect* fragmentation. For *direct* fragmentation the correlation function $C(t)$ will not show an exact exponential decay. For a Gaussian wave function in a linear potential, the decay is approximately Gaussian in time.[38]

C. Relation to kinetics of unimolecular decay

As shown above for indirect fragmentation, the *individual* resonance states decay exponentially in time. This is equivalent to normal first-order reaction kinetics

$$A \rightarrow P, \tag{41}$$

where $[A]/[A]_0 = e^{-kt}$, and $[P]/[A]_0 = 1 - e^{-kt}$.

From the discussion in the previous section it is, however, clear that normally the pump–probe signals will give a result corresponding to a superposition of resonance states. Thus, the product signal is clearly multiexponential. It is, in principle, possible to extract all the individual decay rates, either by a simple multiexponential fitting procedure (provided the signal is known over a sufficiently long time interval) or by more advanced methods.[35] In the special case

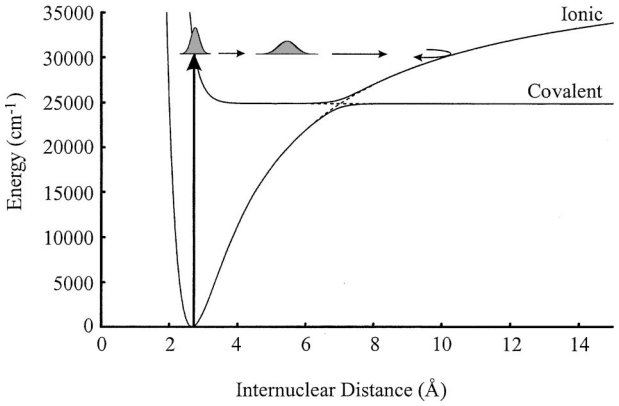

FIG. 1. Potential energy curves for NaI. The solid lines are the adiabatic potentials whereas the dashed lines show the potentials in the diabatic representation. Also shown is the wave packet created by the coherent excitation and an indication of its subsequent dynamics.

where all excited states have the same decay rates, the result in Eq. (30) corresponds to a single exponential rise, $P(t)=1-e^{kt}$.

For sufficiently short times, the product signal can always be described by a single exponential rise

$$P(t)=1-\sum_n |c_n|^2 e^{-k_n t}\sim 1-\left(1-\sum_n |c_n|^2 k_n t\right) =1-e^{-\langle k\rangle t}, \tag{42}$$

in the limit $k_n t \ll 1$, where the average decay rate is defined by $\langle k\rangle=\Sigma_n |c_n|^2 k_n$. That is, from a short time fit to the product signal, we can obtain an average decay rate directly from the pump–probe signal.

It can for sufficiently short times, in some cases, be justified to characterize the decay as bi-exponential. If the dynamics cover two groups of states, one with large decay rates and another with small decay rates, then a better approximation to the short-time behavior of the signal is obtained when Eq. (30) is rewritten to

$$P(t)\sim 1-Ae^{-\langle k\rangle_s t}-Be^{-\langle k\rangle_l t}, \tag{43}$$

where $A=\Sigma_{n=1}^{n=m}|c_n|^2$ and $B=\Sigma_{n>m}|c_n|^2$, and $\langle k\rangle_s=\Sigma_{n=1}^{n=m}|c_n|^2 k_n/A$ is the average decay rate for states with large decay rates (the exponential time dependence is valid only at very short times), and $\langle k\rangle_l=\Sigma_{n>m}|c_n|^2 k_n/B$ is the average decay rate for the states with small decay rates (the corresponding exponential time dependence is valid for somewhat longer times). That is, in this case the product signal can, approximately, be described as bi-exponential.

IV. APPLICATION TO FEMTOSECOND DYNAMICS OF NaI

The experimental and theoretical work on the femtosecond dynamics of NaI is a benchmark illustration of unimolecular dynamics.[14–24] A short pump pulse prepares the molecule on the repulsive wall of a quasi-bound electronic state (see Fig. 1), that is, prepares a vibrating activated molecule,

$$\mathrm{NaI}\xrightarrow{\text{pump}}(\mathrm{NaI})^*\rightarrow \mathrm{Na}+\mathrm{I}, \tag{44}$$

where dissociation is due to nonadiabatic coupling to the lower adiabatic state. The experimental signals show nonkinetic decay and rise of population,[14–16] thus they cannot be described by a single exponential function. The product signal for the rise of Na has ''steps'' spaced with the vibrational period of (NaI)*. The steps arise since the product can only be formed when the wave packet passes the avoided crossing. The pump–probe signal of the activated molecule, (NaI)*, looks very much like a damped autocorrelation function, and the frequency of the resonance recurrences matches that observed for the separation of steps in the product signal.

A number of theoretical studies have been made on this system. For the present discussion we note, in particular, that the lifetimes of a number of the quasi-bound resonance states are known,[24] see Table I and Fig. 2. A large variation in lifetimes is observed and to that end, it has also been observed that the temporal recurrences in the pump–probe signal of the activated molecule, in particular, depends strongly on the parameters of the pump laser.[23,24] We note that the energy levels in Table I (in an energy range corresponding to a pump at 330 nm) are almost evenly spaced with an average spacing of 36 cm^{-1}, which gives a period for the wave packet oscillation of 0.94 ps, in good agreement with experiments.[14–16]

We consider first the description of the pump–probe signals within the framework of decaying resonance states. From the energies and lifetimes in Table I, which correspond to nonoverlapping resonances, we calculate the signals with a Gaussian distribution of the coefficients $|c_n|^2=\exp[-(E_n-\langle E\rangle)^2/\sigma^2]/(\sqrt{\pi}\sigma)$. The distribution is centered at the energy $\langle E\rangle=30\,250\ \mathrm{cm}^{-1}$ corresponding to a pump pulse at 330 nm, with a width given by $\sigma=100\ \mathrm{cm}^{-1}$ (i.e., a pulse duration of about 50 fs). We calculate first the product signal for the rise of Na. From Eq. (30), we obtained the smooth (dashed line) rise shown in Fig. 3(a). Thus, the explanation of the experimentally observed steps is clearly beyond the traditional description of resonance states. The steps are related to the coherent excitation of a number of vibrational states, i.e.,

TABLE I. Energies and widths of resonance states; taken from Ref. 24.

E_n (cm^{-1})	Γ_n (cm^{-1})	E_n (cm^{-1})	Γ_n (cm^{-1})	E_n (cm^{-1})	Γ_n (cm^{-1})
30022.2	0.7236	30202.8	0.2582	30379.3	0.3076
30058.6	0.3354	30238.5	0.6081	30414.4	0.0803
30094.8	0.0946	30274.1	1.1053	30449.4	0.0015
30130.9	0.0013	30308.7	1.1476	30484.2	0.0477
30166.9	0.0558	30344.1	0.6607		

they cannot be accounted for by Eq. (30), but the more accurate expression for the norm, Eq. (24), must be used. In Fig. 3, we have shown the results assuming that the off-diagonal coupling elements are given by Eq. (25) with $\eta_{nn'}$ equal to 1 (if these parameters are chosen to be smaller than 1, the steps will be less pronounced).

The three parts of the figure show the signal for three different choices of the phases of c_n. In (a) $c_n=|c_n|$, (b) $c_n=\exp(in\pi/2)|c_n|$, and (c) $c_n=\exp(in\pi)|c_n|$. These phase relations between the coefficients correspond to $\varphi_{nn'}=0$, $\varphi_{nn'}=(n-n')\pi/2$, and $\varphi_{nn'}=(n-n')\pi$, respectively, in Eq. (24). Since the energy levels in Table I are, essentially, equidistantly spaced, the last two choices translate into the phase shifts of a quarter and half a period, as observed in Figs. 3(b) and 3(c). In passing we note that in a harmonic well, coherent states are formed by a superposition of eigenstates, where the square magnitude of the expansion coefficients follow a Poisson distribution. The phase relation between the expansion coefficients determine the location of the coherent state in the well. With the usual sign convention,[12] positive coefficients result in a coherent state located at the right wall of the harmonic well whereas real coefficients with alternating sign result in a coherent state located at the left wall; a displacement corresponding to one half of an oscillation cycle.

The figures show the observed periodic steps separated by just under a picosecond. Furthermore, Fig. 3(a) shows, in full agreement with the discussion in Sec. III, that the signal averaged over a vibrational period is identical to the signal which is obtained when the coherent interference in the decay of the resonance states is neglected (dashed line). For the purpose of making contact between reaction kinetics and the pump–probe signal obtained in the quasi-bound region, we consider in the following the average signal, that is, neglect the oscillatory terms. We calculate, consequently, the signal associated with the quasi-bound motion using Eq. (33). We choose the Franck–Condon window function to be a Gaussian, Eq. (9), centered at the inner turning point of the adiabatic well at $E=30\,250\,\mathrm{cm}^{-1}$, with the width arising from a probe pulse with the same energy profile as quoted above for the expansion coefficients. Due to the steepness of the inner wall of the adiabatic well, this results in a very narrow window function with a width ~0.1 Å. Within the Franck–Condon window we can, therefore, approximate the resonance states, $\phi_n(r)$, by Airy functions.[11]

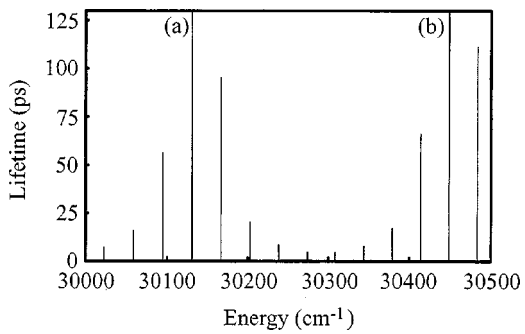

FIG. 2. Distribution of lifetimes according to Table I. The lifetimes of the states marked (a) and (b) are off-scale; 4.1 and 3.5 ns, respectively.

Figure 4(a) shows the signal according to Eq. (33). Also shown is the decay of the average population (norm of the wave packet) in the adiabatic well, which corresponds to unimolecular decay. Thus, the signal decays faster than the norm. In order to describe the decay of the signal, a single exponential fit to the envelope function is shown on the figure. We denote this decay as an apparent decay, since the decay of the signal envelope contains contributions from the unimolecular decay as well as wave packet spreading. Figure 4(b) shows the autocorrelation function (see also Ref. 24). This function is in the present case very similar to the signal since the probe state is centered at the inner turning point of the well and, furthermore, it is highly localized.

According to the discussion in connection with Eq. (38), it is possible to extract information on the time scale of wave packet spreading from the apparent decay [of $S(t)$ or $C(t)$] and the unimolecular decay, at least in the case of a single unimolecular decay rate. We have applied this approach to the results shown in Fig. 4(a), in the following way: The apparent decay has been divided by the decay of the average population. The result is shown in Fig. 4(c) together with the calculated signal where the unimolecular decay is artificially eliminated. Excellent agreement is observed within the first ten vibrational periods. Thus, from the unimolecular decay observed in the average product signal and the pump–probe signal of the quasi-bound motion, we can gain insight into

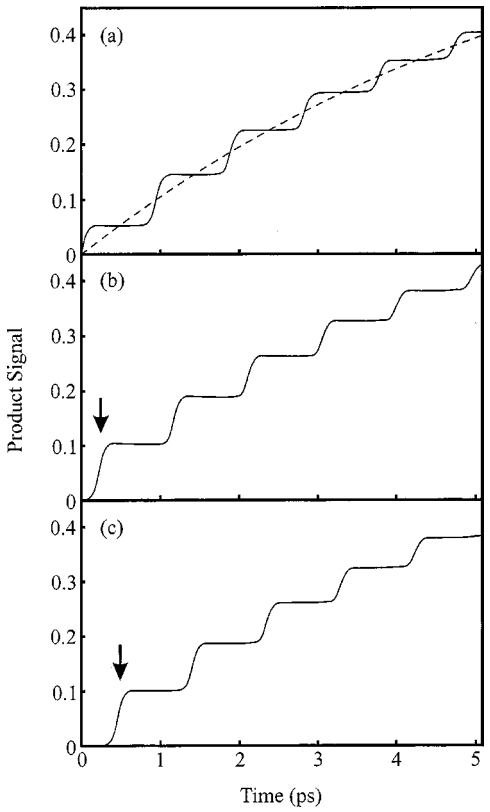

FIG. 3. Product signal for Na+I. The dashed curve corresponds to the situation where interference effects between the quasi-bound vibrational states within the bandwidth of the pump laser are neglected, Eq. (30). The panels (a)–(c) correspond to different choices of the phases for the coefficients representing the initial state, in terms of the resonance states, see text. The arrows in (b) and (c) marks the shift in the induction time, defined as the first time products are observed.

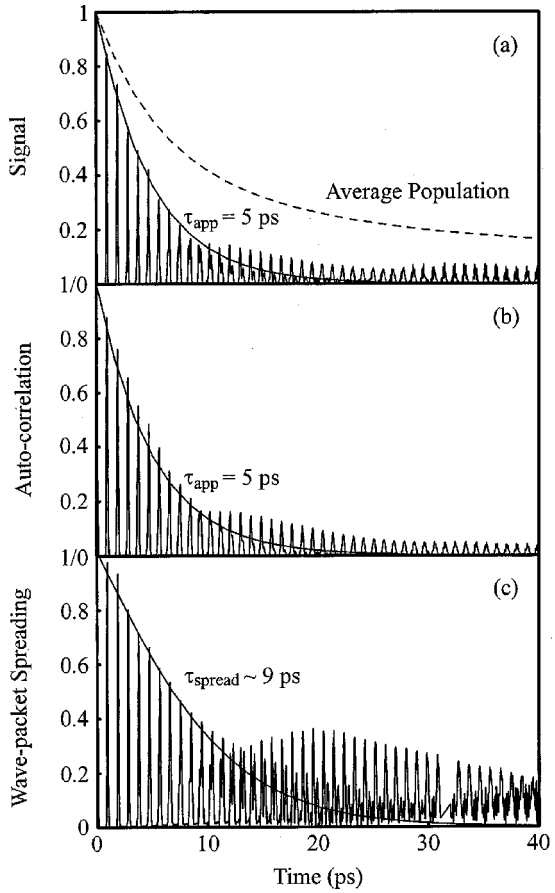

FIG. 4. Pump–probe signal of the transition states. Panel (a) shows the (normalized) signal according to our master equation, Eq. (33): The solid decay curve shows for comparison a single-exponential fit to the decay of the signal, that is, the apparent decay of the signal. The dashed curve shows the average decay of the population in the adiabatic well, Eq. (28). Panel (b) shows the autocorrelation function, Eq. (37): The behavior obtained in panel (a) from our master equation is similarly reproduced by the auto-correlation function. Panel (c) shows the signal obtained when the unimolecular decay is artificially eliminated, noting the enhancement of the recurrences: The decay curve obtained is the ratio between the solid and dashed curves in panel (a). This curve gives the time scale for wave packet spreading of 9 ps (defined as the time when the function has decayed to $1/e$), and the agreement indicates that the peak heights in panel (a) decay by the total rates of average population depletion plus spreading.

the spreading dynamics in the adiabatic well.

Compared to the product signal for the rise of Na, it is more difficult to extract information on the unimolecular decay rates from the pump–probe signal of the quasi-bound motion. As shown above, the overall decay of the signal is not a direct signature of the decay rates of the resonance states. From the theoretical simulations of the signal [Fig. 4(a)], we calculate now the peak areas as a function of time. These areas are constant in the absence of unimolecular decay, according to Eq. (40). We have plotted the areas in Fig. 5. We observe that the areas decay, and they follow closely the decay of the average population of the adiabatic well. Thus, the decay of the peak areas in the signal associated with the quasi-bound motion gives the counterpart of the multiexponential rise of the product signal. The decay of the peak areas has also been studied experimentally.[17] From the experimental signal, it was indeed concluded that the decay of the peak areas correspond to the rise of the product

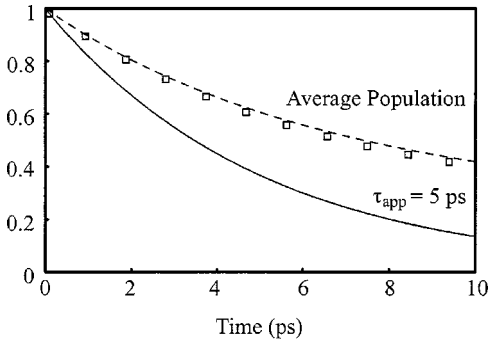

FIG. 5. Decay of the recurrence areas in Fig. 4(a) (squares) compared to decay of the average population in the adiabatic well, Eq. (28) (dashed curve). For comparison, the decay of the envelope in Fig. 4(a) is also drawn (solid line).

signal.[17] Here, the areas decayed by 6 ps, which was found to be similar to the fast rise time of free Na (for a 310 nm pump).

From Table I, it is evident that the decay rates of NaI depends strongly on the energy. This behavior is also found in other systems. For example, detailed calculations on $HO_2 \rightarrow H + O_2$[39] show that, the decay rates of individual resonance states can vary over several orders of magnitude even within a *very* narrow energy range. However, when the rates were convoluted with a Gaussian with a width corresponding to a few hundred cm^{-1}, the rate constant agreed well with the rate constant according to Rice–Ramsperger–Kassel–Marcus (RRKM) theory. Thus, in many situations, knowing all the individual decay rates is simply information which is too detailed and an average rate constant suffices. To that end we showed in Eq. (42) how to extract an average rate constant directly from the pump–probe signals.

Finally, for the unimolecular rate constant in systems like NaI, it has been proposed that the rate constant can be expressed as the frequency of the vibration times the nonadiabatic crossing probability,[8,14] where the probability is evaluated according to the Landau–Zener formula.[11,40] It is worth noting that this relation can be justified from a simple analysis assuming a constant (small) reaction probability, p, in each period of vibration. In this case, the number of reactants, N_t, after n periods can be written

$$N_t = N_0(1-p)^n = N_0 e^{n \ln(1-p)} \sim N_0 e^{-\nu p t}, \tag{45}$$

where we have taken p to be relatively small such that $\ln(1-p) \sim -p$, and that the number of periods corresponds, approximately, to the actual time divided by the period of oscillation, $n \sim t/T = \nu t$. This ($\nu p \equiv k$) is clearly not an expression for a genuine microcanonical rate constant. As shown for NaI (Table I), the decay can depend strongly on the energy of the populated states, and this cannot be explained from the simple representation of the rate constant. Thus the frequency[16] as well as the Landau–Zener probability have a relatively weak dependence on the energy. The proposed relation has indeed only been established for an average rate (averaged over some energy range) in a semiclassical limit.[41]

If we calculate the rate constant according to Eq. (45), using the vibrational period 0.94 ps, which gives the frequency $\nu = 1.06 \cdot 10^{12}\ s^{-1}$, we obtain a rate constant in the

range of $1.06\cdot 10^{11}$ to $1.60\cdot 10^{11}\,s^{-1}$ with a Landau–Zener probability, p, in the range of 0.15–0.1.[18,20] That is, the lifetime is in the range of 6.3–9.4 ps. These numbers are in very good agreement with the average rate constant $\langle k\rangle = \Sigma_n |c_n|^2 k_n$ of Eq. (42), which corresponds to a lifetime of 8.7 ps. For a simulation of the pump–probe signal of NaI with a similar representation of the rate constant, see Refs. 18 and 20.

V. CONCLUSIONS

We considered the relation between pump–probe signals of unimolecular reactions and macroscopic kinetics, that is, the exponential decay of reactants and the exponential rise of the product population, respectively. The description of unimolecular decay used by many authors is originally based on the decay of a single zero-order resonance state. When the decay of a superposition of such states (i.e., a wave packet) is considered, each state has simply been multiplied by its own decay rate. This approach does not reproduce the dynamics and ignores some coherence phenomena. We showed that the pump–probe signals corresponding to unimolecular decay cannot be fully accounted for within this standard approach to unimolecular decay due to vibrational coherence effects between the coherently excited vibrational states. Thus, the resonance states do not decay independently; the decays are coupled via the continuum.

The effect is pronounced on the time-dependent population, in particular the product population which displays an oscillatory modulation around a rising population. When the signal is averaged over a vibrational period, the modulation disappears, and the averaged signal corresponds to a superposition of exponential rises—the kinetic regime. Each exponential reflects the different lifetimes of the quasi-bound states populated by the pump pulse.

Even when all resonance states have the same lifetime, the corresponding exponential decay differ, in general, from the envelope function of the transition state signal due to wave packet spreading. The product signal will, however, show the well-known single exponential rise. Such a behavior, where all resonance states within the bandwidth of the pump laser have approximately the same lifetime, might occur in large molecules with high degree of degeneracy. If this condition is not fulfilled, we showed in this paper how to extract an average rate constant (within the bandwidth of the pump laser) directly from the short time behavior of the pump–probe signals.

We considered the predissociation of NaI as a prototype example, and showed explicitly that all features of the pump–probe signals can be accounted for within the formalism presented in this paper. In particular, the steps in the product signal were reproduced; the average product signal is a multiexponential function which reflects the decay rates of the individual quasi-bound states. The same multiexponential function was found in the decay of the peak areas in the probing of the quasi-bound motion. The relationship of these decay processes to the Landau–Zener average rate of crossing was examined and related to experimental observables.

ACKNOWLEDGMENTS

This work was supported by the National Science Foundation, and U.S. Air Force Office of Scientific Research. N.E.H. appreciates the hospitality he has experienced during his visit to Caltech and LMS.

[1] A. H. Zewail, *Femtochemistry: Ultrafast Dynamics of the Chemical Bond* (World Scientific, Singapore, 1994).
[2] *Femtosecond Chemistry*, edited by J. Manz and L. Wöste (VCH, Weinheim, 1995).
[3] *Femtochemistry*, edited by M. Chergui (World Scientific, Singapore, 1996).
[4] *Femtochemistry and Femtobiology: Ultrafast Reaction Dynamics at Atomic-Scale Resolution*, edited by V. Sundström (Imperial College Press, London, 1997).
[5] A. W. Castleman, Jr., and V. Sundström, J. Phys. Chem. A **102**, 4021 (1998).
[6] A. H. Zewail, J. Phys. Chem. A **104**, 5660 (2000).
[7] R. Schinke, *Photodissociation Dynamics* (Cambridge University Press, Cambridge, 1993).
[8] T. Baer and W. L. Hase, *Unimolecular Reaction Dynamics* (Oxford University Press, Oxford, 1996).
[9] V. Engel and H. Metiu, J. Chem. Phys. **95**, 3444 (1991).
[10] R. D. Levine, *Quantum Mechanics of Molecular Rate Processes* (Oxford University Press, London, 1969).
[11] L. D. Landau and E. M. Lifshitz, *Quantum Mechanics*, 3rd ed. (Pergamon, Oxford, 1977).
[12] C. Cohen-Tannoudji, B. Diu, and F. Laloë, *Quantum Mechanics* (Wiley, New York, 1977).
[13] M. Bixon and J. Jortner, J. Chem. Phys. **107**, 1470 (1997).
[14] T. S. Rose, M. J. Rosker, and A. H. Zewail, J. Chem. Phys. **88**, 6672 (1988).
[15] M. J. Rosker, T. S. Rose, and A. H. Zewail, Chem. Phys. Lett. **146**, 175 (1988).
[16] T. S. Rose, M. J. Rosker, and A. H. Zewail, J. Chem. Phys. **91**, 7415 (1989).
[17] P. Cong, A. Mokhtari, and A. H. Zewail, Chem. Phys. Lett. **172**, 109 (1990).
[18] P. Cong, G. Roberts, J. L. Herek, A. Mohktari, and A. H. Zewail, J. Phys. Chem. **100**, 7832 (1996).
[19] V. Engel, H. Metiu, R. Almeida, R. A. Marcus, and A. H. Zewail, Chem. Phys. Lett. **152**, 1 (1988).
[20] S.-Y. Lee, W. T. Pollard, and R. A. Mathies, J. Chem. Phys. **90**, 6146 (1989).
[21] V. Engel and H. Metiu, J. Chem. Phys. **90**, 6116 (1989).
[22] V. Engel and H. Metiu, J. Chem. Phys. **91**, 1596 (1989).
[23] C. Meier, V. Engel, and J. S. Briggs, J. Chem. Phys. **95**, 7337 (1991).
[24] S. Chapman and M. S. Child, J. Phys. Chem. **95**, 578 (1991).
[25] J. Cao and K. R. Wilson, J. Chem. Phys. **106**, 5062 (1997).
[26] S.-Y. Lee, W. T. Pollard, and R. A. Mathies, Chem. Phys. Lett. **163**, 11 (1989); S.-Y. Lee, in Ref. 2.
[27] Y. J. Yan and S. Mukamel, Phys. Rev. A **41**, 6485 (1990).
[28] H. Dietz and V. Engel, J. Phys. Chem. A **102**, 7406 (1998).
[29] M. Hillery, R. F. O'Connell, M. O. Scully, and E. P. Wigner, Phys. Rep. **106**, 121 (1984).
[30] Z. Li, Y.-L. Fang, and C. C. Martens, J. Chem. Phys. **104**, 6919 (1996).
[31] M. S. Child, *Molecular Collision Theory* (Dover, New York, 1996).
[32] *Dynamics of Molecules and Chemical Reactions*, edited by R. E. Wyatt and J. Z. H. Zhang (Marcel Dekker, New York, 1996).
[33] K. Museth and C. Leforestier, J. Chem. Phys. **104**, 7008 (1996).
[34] Q. Liu, C. Wan, and A. H. Zewail, J. Phys. Chem. **100**, 18666 (1996).
[35] S. K. Gray, J. Chem. Phys. **96**, 6543 (1992).
[36] E. J. Heller, J. Chem. Phys. **62**, 1544 (1975).
[37] K. B. Møller and N. E. Henriksen, J. Chem. Phys. **105**, 5037 (1996).
[38] N. E. Henriksen, Adv. Chem. Phys. **91**, 433 (1995).
[39] A. J. Dobbyn, M. Stumpf, H. Keller, and R. Schinke, J. Chem. Phys. **104**, 8357 (1996).
[40] N. E. Henriksen, Chem. Phys. Lett. **197**, 620 (1992).
[41] E. J. Heller and R. C. Brown, J. Chem. Phys. **79**, 3336 (1983).